

# FLRQ: Faster LLM Quantization with Flexible Low-Rank Matrix Sketching

Hongyaoxing Gu<sup>1,2</sup>, Lijuan Hu<sup>1</sup>, Shuzi Niu<sup>1</sup>, Fangfang Liu<sup>1,3\*</sup>

<sup>1</sup>Institute of Software Chinese Academy of Sciences

<sup>2</sup>University of Chinese Academy of Sciences

<sup>3</sup>Key Laboratory of System Software (Chinese Academy of Sciences)

## Abstract

Traditional post-training quantization (PTQ) is considered an effective approach to reduce model size and accelerate inference of large-scale language models (LLMs). However, existing low-rank PTQ methods require costly fine-tuning to determine a compromise rank for diverse data and layers in large models, failing to exploit their full potential. Additionally, the current SVD-based low-rank approximation compounds the computational overhead. In this work, we thoroughly analyze the varying effectiveness of low-rank approximation across different layers in representative models. Accordingly, we introduce Flexible Low-Rank Quantization (FLRQ), a novel solution designed to quickly identify the accuracy-optimal ranks and aggregate them to achieve minimal storage combinations. FLRQ comprises two powerful components, Rank1-Sketch-based Flexible Rank Selection (R1-FLR) and Best Low-rank Approximation under Clipping (BLC). R1-FLR applies the R1-Sketch with Gaussian projection for the fast low-rank approximation, enabling outlier-aware rank extraction for each layer. Meanwhile, BLC aims at minimizing the low-rank quantization error under the scaling and clipping strategy through an iterative method. FLRQ demonstrates strong effectiveness and robustness in comprehensive experiments, achieving state-of-the-art performance in both quantization quality and algorithm efficiency.

## Introduction

Large language models (LLMs) have demonstrated outstanding capabilities across a wide range of tasks that significantly impact our daily lives. However, the scale of LLMs makes their deployment extremely challenging, necessitating quantization techniques for reducing model size while improving inference efficiency (Kuzmin et al. 2023).

In quantization methods, Quantization-Aware Training (QAT) incorporates pseudo-quantization layers to simulate the quantization process (Liu et al. 2024), requiring retraining with different quantization parameters. This approach inevitably demands higher computational costs and can be affected by modifications to the original model architecture. In contrast, Post-Training Quantization (PTQ) has recently gained more attention for a faster quantization process and

\*Corresponding author

Accepted as a poster paper in AAAI 2026

Method	Rank	Lora func
LoRC(Yao et al. 2024)	1,4,8,16,32	SVD
LoftQ(Li et al. 2024b)	16,32	SVD
LQER(Zhang et al. 2024)	600	SVD
$L^2$ QER(Zhang et al. 2024)	32,64,256	SVD
SVD-Quant(Li et al. 2024a)	16,32,64	SVD
FLRQ(ours)	Flexible	R1-Sketch

Table 1: Previous low-rank quantization methods are constrained to restricted low-rank components, while FLRQ under R1-Sketch provides the flexibility to select effective low-rank approximations, thereby minimizing computational resource wastage and achieving high efficiency.

state-of-the-art PTQ methods have achieved accuracy comparable to QAT (Ding et al. 2022; Hubara et al. 2021; Frantar et al. 2023). Among post-training quantization (PTQ) methods, low-rank approaches have garnered significant attention in recent years due to their effectiveness in capturing essential weight information, thereby enhancing quantization accuracy.

Current low-rank quantization approaches typically adopt a fixed rank and apply it uniformly across all layers of a model. However, recent studies reveal that different layers exhibit varying degrees of importance. This uniform-rank strategy has two primary drawbacks: 1. For models of different sizes, the memory usage ratio under the same rank varies, necessitating separate tuning of the fixed rank for each model; 2. A fixed rank leads to inconsistent effectiveness in capturing weight feature across layers, resulting in potential memory waste and insufficient performance.

Given these issues, we have proposed an iterative FLRQ method for flexible rank selection in different layers of the model, which is also shown in Figure 1. Furthermore, we enhance the matrix sketching algorithm to accelerate our proposed method. Our key contributions are as follows.

- We analyzed the effectiveness of reducing error in different layers of large model weights under low-rank approximation, and proposed FLRQ for selecting optimal low-rank components across various layers, which does not require expensive knowledge distillation, hyperparameter search, and is easily integrated with other approaches.

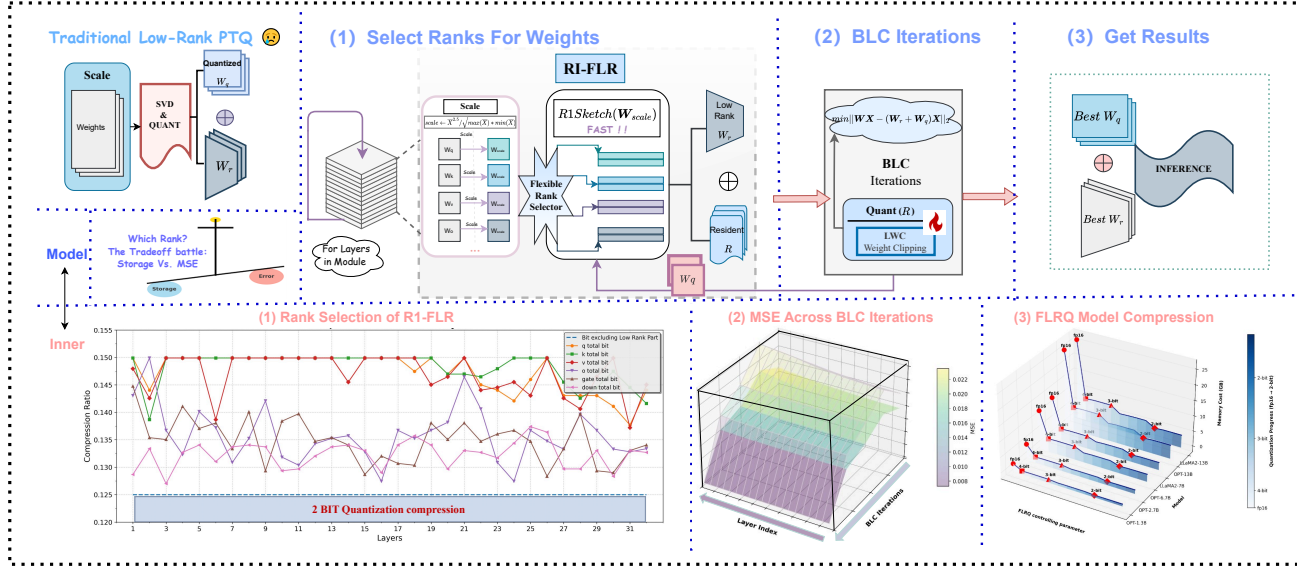


Figure 1: The presentation at the model layer and internals of FLRQ, (1) to (3) represent the three steps of the FLRQ algorithm respectively. In detail, FLRQ utilizes flexible rank selections (1), activation-based scaling, and iterative Best Low-rank Approximation under Clipping (BLC) algorithm (2), leading to higher quantization accuracy and smaller model size (3).

- We proposed rank-1 sketch (R1-Sketch) under Gaussian projection by reformulating the randomized SVD algorithm and carrying efficient implementation on GPU platform. This technique is suited for low-rank component extraction and solely utilizes BLAS Level-2 routines, ensuring highly efficient computations.
- Experiments demonstrate that FLRQ achieves comparable accuracy with fewer memory costs and outperforms conventional schemes by a significant margin in accuracy, especially for low-bit precision (INT2). Moreover, the R1-Sketch method effectively reduces computation time and has low inference latency.

## Background and Related Work

### Post-Training Quantization

PTQ (Post-Training Quantization), as a technique for model compression, has received extensive attention in recent years: Weight-only quantization in PTQ can be expressed as

$$\mathbf{O} = \text{Quant}(\mathbf{W}) \cdot \mathbf{X}. \quad (1)$$

AWQ (Lin et al. 2024) enhances the quantization accuracy by preserving the top 1% of significant activation channels by applying a scale matrix. GPTQ (Frantar et al. 2023) quantizes each parameter by OBS (Hassibi, Stork, and Wolff 1993) per block to mitigate the accuracy loss from quantization.

Recent studies like Omnipoint (Shao et al. 2023) introduced learnable weight clipping, Quip# (Tseng et al. 2024) employs a randomized matrix transformation, while Affinequant (Ma et al. 2024) uses equivalent affine transformations, CALDERA (Saha et al. 2024) applies low-rank decomposition in quantization. These methods consider the challenging regime of sub-4 bit post-training LLM quantization but there are still challenges for 2-bit quantization.

### Low-Rank methods in LLMs quantization

Low-rank methods in quantization have attracted considerable attention in recent years. Low-rank quantization takes advantage of the low-rank decomposition of the weight quantization matrix (Yao et al. 2024), followed by residual quantization represented as:

$$\mathbf{W}\mathbf{X} = (\text{Quant}(\mathbf{W} - \mathbf{W}_r) + \mathbf{W}_r)\mathbf{X}, \quad (2)$$

where the rank  $r$  matrix  $\mathbf{W}_r$  is the low-rank approximation of  $\mathbf{W}$  with minimal error, which can be calculated by SVD (Singular value decomposition):

$$\mathbf{W}_r = \text{SVD}(\mathbf{W}) = (\mathbf{U}_r \mathbf{\Sigma}_r \mathbf{V}^T) = \mathbf{W}_L \mathbf{W}_R. \quad (3)$$

A small subset of high singular value components can be isolated, and extracting these low-rank matrices effectively reduces the impact of outliers. This approach is broadly categorized into two types:

- **low-rank within quantization:** The former belongs to post-training quantization (PTQ) methods, where low-rank approximation is applied during quantization to reduce weight outliers and thereby minimize quantization error. For instance, ViTALiTy (Dass et al. 2023) employs a combination of sparsification and low-rank approximation, while LQER (Zhang et al. 2024) integrates Block Floating Point techniques to further enhance accuracy. Similarly, SVD-Quant (Li et al. 2024a) introduces low-rank methods into diffusion models, yielding significant performance improvements.
- **low-rank fine-tuning after quantization:** This involves refining the PTQ quantized model on a dataset to improve accuracy, as exemplified by methods such as LoftQ (Li et al. 2024b) achieves nearly lossless inference quantization by designing tailored singular value distributions.

Recent work like CALDERA (Saha et al. 2024) improves L2-loss by iteration and applies mix-precision in  $\mathbf{W}_r$ , and RILQ (Lee et al. 2025) considers the construct of  $\mathbf{W}_r$  by model loss instead of linear loss, both methods perform low-rank fine-tuning based on state-of-the-art PTQ like Omnipoint (Shao et al. 2023) and achieve high-precision 2-bit models on QUIP# (Tseng et al. 2024).

### Sketching matrix and RSVD algorithm

Matrix sketching is a technique designed to efficiently handle large-scale matrices. Its core idea is to construct a “sketch” through randomization. This approach reduces storage and computational costs while preserving most of the essential information. Randomized Singular Value Decomposition (RSVD) (Halko, Martinsson, and Tropp 2011) represents one class of matrix sketching techniques utilized for low-rank approximation and has been widely applied in computer vision (Ji and Li 2014; Osawa et al. 2017) and machine learning (Guan, Li, and Guan 2017; Kumar 2016). This algorithm is generally divided into the following two steps:

1. Compute an approximate basis for the column space of  $A \in \mathbb{R}^{m \times n}$ , assume  $m \leq n$ . Attempt it in  $it$  times to obtain a matrix  $Q$  with  $r$  orthogonal columns that approximates matrix  $A$ . Formally,  $A_r \approx QQ^*A$ , where  $Q^*$  denotes the conjugate transpose of  $Q$ .
2. Utilize the orthogonal matrix  $Q$  to calculate a much smaller rank- $k$  matrix  $Q^*A$ , and employ it to compute the desired low-rank matrix by Singular Value Decomposition.

It is evident that the computational requirements for RSVD are significantly reduced compared to SVD and the error satisfies<sup>1</sup>:

$$\mathbb{E}\|A - A_r\| \leq \sigma_{r+1} + \left[1 + 4\sqrt{\frac{2n}{r-1}}\right]^{1/(it+1)} \sigma_{r+1}. \quad (4)$$

where  $\sigma_i$  represents the  $i$ -th largest singular value of  $A$ .

### Motivation: Why do we need flexible and fast rank selection?

In Low-rank methods, rank selection often relies on empirical insights in specific layers, and the selected rank is a fixed value for all weights. For example, LoRC in ZeroQuant2 (Yao et al. 2024) fixes the rank as  $2^n$ , RILQ and LoftQ use fixed ranks of 16 or 32, and experiments in LQER suggest that a rank of 64 is sufficient to maintain the accuracy of the OPT-1.3b model, SVD-Quant adopts a fixed rank of 32 while CALDERA applies ranks from 64 to 256.

A fixed rank introduces non-negligible memory and latency costs. Under 2-bit quantization, LQER with rank 256 incurs roughly **50%** additional memory, whereas CALDERA with rank 256, despite achieving higher accuracy, it brings 20% extra memory and increasing inference latency by nearly **30%** on 7B model. The overhead of SVD or fine-tuning-based quantization is also substantial: RILQ demonstrates competitive accuracy at rank 16 yet must be combined

<sup>1</sup>The proof of this theorem is complex; for specifics, one may refer to (Halko, Martinsson, and Tropp 2011).

with other quantization methods—e.g., RILQ+OmniQuant requires 3.1 h for quantization and about 1 h for fine-tuning on LLaMA2-7B and SVD-based methods severely slow quantization, diminishing usability.

## Method

In quantization, low-rank methods frequently employ a fixed rank approach, which is not ideally suited for all layers. We introduce **FLRQ** (Flexible Low-Rank Quantization), structured into two primary components and presented in Algorithm 2:

- **R1-FLR** (R1-Sketch-based Flexible Rank Selection): This component focuses on dynamically determining the rank for each layer under rank-1 sketch (R1-Sketch), allowing for adaptability according to the specific characteristics and requirements of individual layers.
- **BLC** (Best Low-rank Approximation under Clipping): This segment aims at achieving efficient low-rank approximations when utilizing clipping strategies to minimize quantization errors while preserving critical data features.

In this section, we will first present the R1-Sketch algorithm, followed by the introduction of two optimization methods: **R1-FLR** and **BLC**.

### Low rank under R1-Sketch

To address the inefficiency of SVD, we proposed a simplification to the randomized SVD (RSVD) algorithm under the rank-1 condition. This simplification introduces a rank-1 matrix approximation technique, as described in below:

Given a matrix  $A \in \mathbb{R}^{m \times n}$ . For a standard RSVD (Randomized Singular Value Decomposition) algorithm prototype, it typically consists of the following two steps:

#### Stage A:

1. Generate an  $\mathbb{R}^{n \times r}$  Gaussian test matrix  $S$ .
2. Form  $\mathbf{Y} = (\mathbf{A}\mathbf{A}^*)^{it}\mathbf{A}S$ .
3. Construct a matrix  $\mathbf{Q} = QR(\mathbf{Y})$  by QR decomposition whose columns form an orthonormal basis of  $\mathbf{Y}$ .

#### Stage B:

1. Form  $\mathbf{B} = \mathbf{Q}^*A$ .
2. Compute an SVD of the small matrix:  $\mathbf{B} = \mathbf{U}\Sigma\mathbf{V}^*$ .
3. Set  $\mathbf{U} = \mathbf{Q}\mathbf{U}$ .

If a rank-1 matrix  $\mathbf{S} \in \mathbb{R}^{n \times 1}$  is utilized for low-rank approximation of a matrix, substitute the rank-1 matrix in the two stages, we also have  $\mathbf{Y} = (\mathbf{A}\mathbf{A}^*)^{it}\mathbf{A}S$ .

then for the matrix  $\mathbf{Y} \in \mathbb{R}^{m \times 1}$ , the QR decomposition can be directly represented as follows.

$$\mathbf{Q} = \frac{\mathbf{Y}}{\|\mathbf{Y}\|} \in \mathbb{R}^{m \times 1}, \mathbf{R} = \|\mathbf{Y}\| \in \mathbb{R}^{1 \times 1}. \quad (5)$$

Similarly, the SVD decomposition for rank-1 matrix  $\mathbf{B} = \mathbf{Q}^*A$  can be represented as follows:

$$\mathbf{U} = \{1\}, \Sigma = \|\mathbf{B}\|, \mathbf{V} = \frac{\mathbf{B}}{\|\mathbf{B}\|}. \quad (6)$$

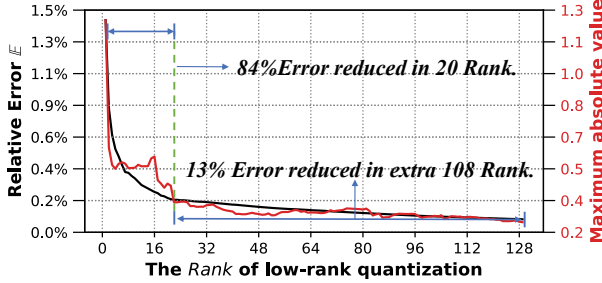


Figure 2: As the extraction rank increases, the curves of the relative error  $\mathbb{E}$  under  $L_2$  norm and the  $amax$  value decrease.

Denote  $A_L = Q\mathbf{U}\Sigma$  and  $A_R = \mathbf{V}$ . Apply the results of SVD decomposition, we have:

$$\begin{aligned} A_L &= \frac{(\mathbf{A}\mathbf{A}^*)^{it}\mathbf{A}\mathbf{S}}{\|(\mathbf{A}\mathbf{A}^*)^{it}\mathbf{A}\mathbf{S}\|} \cdot \frac{\|\mathbf{S}^*\mathbf{A}^*(\mathbf{A}\mathbf{A}^*)^{it}\mathbf{A}\|}{\|(\mathbf{A}\mathbf{A}^*)^{it}\mathbf{A}\mathbf{S}\|}, \\ A_R &= \frac{\mathbf{B}}{\|\mathbf{B}\|} = \frac{\mathbf{S}^*\mathbf{A}^*(\mathbf{A}\mathbf{A}^*)^{it}\mathbf{A}}{\|\mathbf{S}^*\mathbf{A}^*(\mathbf{A}\mathbf{A}^*)^{it}\mathbf{A}\|}. \end{aligned} \quad (7)$$

### R1-Sketch-based Flexible Low-Rank Selection

Given a layer  $\mathbf{W} \in \mathbb{R}^{m \times n}$  in  $d_{fp}$  and perform a pseudo-quantization with  $r$  rank  $\mathbf{W}_r$  under  $d$  bit.

$$\widehat{\mathbf{W}}_q = \text{clamp}(\lfloor \mathbf{R}/s_r \rfloor) * s_r; s_r = \frac{2^{d-1}-1}{\text{amax}(\mathbf{R})}, \quad (8)$$

where  $\mathbf{R} = \mathbf{W} - \mathbf{W}_r$ . Then  $\widehat{\mathbf{W}}$  can be decomposed into  $\widehat{\mathbf{W}} = \widehat{\mathbf{W}}_q + \mathbf{W}_r$ . The low-rank component is stored in original precision which is nearly lossless.

As a example illustrated in Figure 2, the quantization error  $\mathbb{E} = \|\mathbf{W}\mathbf{X} - \widehat{\mathbf{W}}\mathbf{X}\|/\|\mathbf{W}\mathbf{X}\|$  gradually decreases as the rank increases. However, repeated recalculation of  $\mathbb{E}$  after layer re-quantization following rank adjustments incurs significant computational costs. In order to improve quantization efficiency, we propose a flexible rank selection approach based on  $amax$  aimed at minimizing quantization errors while optimizing computational efficiency.

Assume that the corresponding  $amax$  for this rank is  $w_r$ . Then the maximum quantization error under rank  $r$  quantization is  $E_r = \frac{1}{2s_r}$ . Thus, the error reduced by  $p = \frac{E_0}{E_r} = \frac{w_0}{w_r}$ , the precision improvement corresponding to an additional  $d' = \log_2(p)$  bits. Consequently, the model bit-width increases to  $d + d'$ , and the effective quantization bits increase by  $q$  in Eq.9; For memory costs, after incorporating rank- $r$  matrix, the model size increased by  $k$  in Eq.9.

$$q = \frac{d + d'}{d}, k = 1 + \frac{d_{fp} \times r \times (m + n)}{d \times m \times n}. \quad (9)$$

Then, **R1-FLR** workflow is as follows, and shown in Algorithm 1:

Starting the traversal of  $r$  from 1, applying the R1-Sketch method for computing the low-rank matrix corresponding to the current rank-1 matrix, then utilizing Equation 9 to calculate the parameters  $q$  and  $k$  during each iteration.

Algorithm 1: R1-Sketch Flexible Low-Rank Selection (R1-FLR)

---

**Data:**  $W \in \mathbb{R}^{m \times n}$ (weight),  $X$ (value from calibration,)

**Result:**  $W_r, W_q$

Begin **R1-FLR** processes:

**for**  $i = 1$  to  $n$  **do**

- Obtain the sketch rank-1 matrix by Eq.13:
- $\{\mathbf{U}_1, \mathbf{V}_1\} \leftarrow \text{calR1matrix}(\mathbf{R})$ ;
- $\mathbf{R} \leftarrow \mathbf{R} - \mathbf{U}_1 \cdot \mathbf{V}_1$ ;
- get  $amax$  now:  $maxAbs \leftarrow \text{amax}(\mathbf{R})$ ;
- Calculate  $Q, K$  by Eq.9 and the slope:
- $sNow \leftarrow \text{getSlope}(maxAbs)$ ;
- if**  $K > Q$  or  $K > 1 + x$  or  $sNow < t$  **then**

  - | Endloop;

- end**

**end**

**return**  $W_L, W_R$ ;

---

1. If  $q > k$ , it demonstrates that the precision improvement achieved exceeds the increase in model size. Thus, the r-rank quantization is effective.
2. If  $q \leq k$ , it indicates that the precision improvement achieved is not larger than the increase in model size due to the extraction of low-rank components.

### Best Low-rank Approximation under Clipping

**Low-rank quantization with calibration:** Recent studies have shown that the data distribution of activation can influence the effectiveness of quantization Lin et al. (2024); Zhang et al. (2024). Scaling the weights according to the activation values can significantly reduce quantization errors. Specifically, this involves using a calibration dataset to perform inference on each layer during quantization to obtain the current layer's activation value distribution, then calculating a scale vector that is applied before low-rank approximation, which can perform as:

$$\{\mathbf{U}', \mathbf{V}\} = \text{R1-FLR}(\alpha \mathbf{W}), \quad \mathbf{U} = \alpha^{-1} \mathbf{U}'. \quad (10)$$

The calculation of  $\alpha$  is:

$$\alpha = \overline{\mathbf{X}}^{2.5} / \sqrt{\text{max}(\overline{\mathbf{X}}) * \text{min}(\overline{\mathbf{X}})}, \quad (11)$$

where  $\mathbf{X}$  is the corresponding activation value of  $\mathbf{W}$  and  $\overline{\mathbf{X}}$  is per-token normalized mean of  $\mathbf{X}$ . The calculation here is similar to that in AWQ (Lin et al. 2024). In addition, during quantization, setting a portion of the numbers with the largest absolute values to zero by clipping can improve quantization accuracy.

**Get best low-rank quantization by iteration:** With the aforementioned strategies, the algorithm flow is as follows:

1. Under calibration, use R1-FLR to compute the low-rank matrix with scaling to obtain  $\mathbf{W}_r$ .
2. Apply clipping to find a  $p_{clp}$  and cut off the elements whose absolute values exceed  $p_{clp}$ , where  $\mathbf{W}_{clp} = \text{Clipping}(\mathbf{W} - \mathbf{W}_r, p_{clp})$ .

Precision	Method	OPT-1.3b		OPT-6.7b		OPT-13b		LLaMA2-7b		LLaMA2-13b	
		Wiki	C4	Wiki	C4	Wiki	C4	Wiki	C4	Wiki	C4
FP16	Baseline	14.62	14.72	10.86	11.74	10.13	11.19	5.47	6.97	4.88	6.47
W4A16	RTN	31.96	21.45	12.05	13.37	11.41	12.41	5.88	7.30	5.12	6.60
	AWQ	15.22	15.04	10.93	11.87	10.21	11.28	5.61	7.13	4.97	6.56
	OmniQuant	14.88	15.03	10.96	11.85	10.20	11.29	5.58	7.12	4.95	6.56
	AffineQuant	14.79	14.98	10.92	11.84	10.19	11.27	5.58	7.12	4.95	6.56
W3A16	FLRQ	<b>14.65↓</b>	<b>14.97↓</b>	<b>10.84↓</b>	<b>11.84↓</b>	<b>10.13↓</b>	<b>11.28↓</b>	<b>5.55↓</b>	<b>7.06↓</b>	<b>4.94↓</b>	<b>6.52↓</b>
	RTN	119.1	126.47	23.54	32.56	46.03	44.12	6.66	8.4	5.51	7.18
	AWQ	16.32	16.27	11.41	12.30	10.68	11.61	6.24	7.84	5.32	6.94
	OmniQuant	15.72	16.11	11.27	12.31	10.47	11.63	6.03	7.75	5.28	6.98
	AffineQuant	15.61	<b>16.02</b>	11.18	<b>12.21</b>	10.51	11.63	6.08	7.83	5.28	6.99
W2A16	FLRQ	<b>15.53↓</b>	<b>16.07</b>	<b>11.18↓</b>	<b>12.37</b>	<b>10.52↓</b>	<b>11.68↓</b>	<b>5.88↓</b>	<b>7.45↓</b>	<b>5.16↓</b>	<b>6.77↓</b>
	RTN	1.3e4	7.7e3	7.8e3	5.2e3	7.6e4	2.8e4	4.2e3	4.9e3	122.2	139.6
	AWQ	47.97	38.40	16.2	16.48	14.32	14.73	2.2e5	1.7e5	1.2e5	9.4e4
	OmniQuant	23.95	27.33	14.43	16.67	12.94	14.92	11.06	15.02	8.26	11.05
	AffineQuant	23.32	23.28	14.18	15.62	12.88	14.60	10.87	13.13	7.64	10.32
	FLRQ	<b>22.99↓</b>	<b>22.52↓</b>	<b>14.05↓</b>	<b>15.23↓</b>	<b>12.60↓</b>	<b>13.81↓</b>	<b>9.14↓</b>	<b>12.10↓</b>	<b>6.77↓</b>	<b>8.87↓</b>

Table 2: WikiText2 and C4 perplexity (PPL ↓) results on OPT and LLaMA-2 models, context length is 2048.

Algorithm 2: Flexible Low-Rank Matrix Sketching Quantization

```

Data:  $W \in \mathbb{R}^{m \times n}$ (weight),  $X$ (value from calibration)
Result:  $W_r, W_q$ 
Init quantization:  $W_r = SVD(W)$ ,
 $W_q = Quant(W - W_r)$ ,  $bestE \leftarrow inf$ ;
Start BLC processes;
for  $i = 1$  to epochs do
     $\mathbb{E} \leftarrow ||W\mathbf{X} - (W_r + W_q)\mathbf{X}||_2$ ;
    if  $\mathbb{E} < minE$  then
         $minE \leftarrow \mathbb{E}$ ;
         $\{bestW_r, bestW_q\} \leftarrow \{W_r, W_q\}$ ;
    end
    Calculate the resident matrix:  $R \leftarrow W - W_q$ ;
     $W_r = \{W_L, W_R\} \leftarrow R1-FLR(R)$ ;
    Apply weight clipping to rest of  $W$ :
     $W_{clp} \leftarrow Clipping(W - W_r, p_{clp})$ ;
    Quantize the  $W_{clp}$ :  $W_q = Quant(W_{clp})$ ;
end
return  $bestW_r, bestW_q$ ;

```

3. Quantize the clipped matrix  $W_q = Quant(W_{clp})$ .

In this context, is such a decomposition optimal? Considering this from error under  $L_2$  norm, we aim to find a  $d$  bit quantized matrix  $W_q$  and a rank  $r$  matrix  $W_r$  that minimize

$$\min_{r, p_{clp}} \left[ \mathbb{E} ||W\mathbf{X} - (W_r + W_q)\mathbf{X}||_2 \right]. \quad (12)$$

Since the original problem is non-trivial and difficult to solve directly, we propose an iterative method **BLC** to progressively compress the residual space between the low-rank quantization and the original weights, thereby obtaining a

minimized error. The core strategy of **BLC** involves the alternating update of  $W_r$  and  $p_{clp}$ . Firstly, we apply **R1-FLR** and clipping to obtain  $W_r$  and  $W_q$ . Then loop through the following three operations below to find the  $W_q$  and  $W_r$  corresponding to the minimum error  $\mathbb{E}$ :

1. Calculate  $\mathbb{E} = ||W\mathbf{X} - (W_r + W_q)\mathbf{X}||_2$ .
2. Calculate the quantized residual matrix  $R = W - W_q$  and obtain  $W_r = \mathbf{R1-FLR}(R)$ .
3. Apply **clipping** to find  $p'_{clp}$  for clipping and  $W_q = Quant(Clipping(W - W_r, p'_{clp}))$ .
4. Update the  $W_q, W_r$  corresponding to the minimum  $\mathbb{E}$ .

Now we present FLRQ algorithm, which incorporates the BLC iteration and R1-FLR flexible rank selection and the pseudo-code is shown in Algorithm 2.

## Experiments

**SetUp:** We performed a series of evaluations on FLRQ. During quantization, the hyperparameter  $it$  at 2 in main evaluations and the group size was fixed at 128, aligning with the settings in AWQ quantization (Shao et al. 2023). All experiments were conducted on an Nvidia A100 40G GPU. Our evaluations included perplexity and zero-shot tests in the OPT (Zhang et al. 2022), LLaMA-2 and LLaMA-3 (Touvron et al. 2023) model families for language generation tasks.

**Baselines:** We used AWQ (Lin et al. 2024), LQER (Zhang et al. 2024), OmniQuant (Shao et al. 2023) and Affinequant (Ma et al. 2024) as the primary baselines for comparison.

**Evaluation Tasks:** For the evaluation tasks, we conducted perplexity experiments on the WikiText2 (Merity et al. 2016)

Bit	OPT			LLaMA2	
	1.3B	6.7B	13B	7B	13B
4	30.5/0.34	27.1/0.16	27.0/0.12	36.1/0.21	38.6/0.18
3	28.8/0.33	27.7/0.16	26.4/0.12	35.8/0.21	38.4/0.18
2	27.6/0.33	32.7/0.19	33.6/0.15	39.2/0.24	41.9/0.20

Table 3: The extracted rank and extra average bit width of FLRQ at different  $x$  values as (rank/extra-avg.bit).

Bit	Method	extra.bit $\downarrow$	avg.rank $\downarrow$	Wiki2 $\downarrow$	C4 $\downarrow$
3	LQER	0.21	32	6.23	8.82
	FLRQ	0.23	36	<b>5.88</b>	<b>7.45</b>
2	LQER	1.60	256	10.33	12.12
	FLRQ	0.24	39	<b>9.14</b>	<b>12.10</b>

Table 4: Compare with LQER on LLaMA2-7b.

and C4 (Raffel et al. 2020) datasets. We performed zero-shot experiments using test sets including ARC(challenge,easy) (Boratko et al. 2018), BOOLQ (Clark et al. 2019), OpenBookQA (Mihaylov et al. 2018), PIQA (Bisk et al. 2020), and Winogrande (Sakaguchi et al. 2021), with the lm-evaluation-harness (Gao et al. 2024) framework testing.

## Language Generation

We tested FLRQ on model perplexity at 4,3,2-bit. The results are presented in Table 2 and the memory costs are shown in Table 3. According to the results, FLRQ outperforms four PTQ methods on most tasks. Then we compared FLRQ with LQER and the results are presented in Table 4. In LQER’s 2-bit quantization, a significantly high fixed rank of 256 is required to maintain accuracy, whereas in FLRQ, the average rank at 2-bit is only around 40, achieving better perplexity. This is attributed to our flexible rank selection and BLC method, which reduces the residual space thereby making our approach superior to non-iterative methods with fixed ranks as shown in Figure 1.(2).

Recently, low-rank quantized fine-tuning algorithms have received widespread attention. We compare our approach with two fine-tuning methods, CALDERA and RILQ, both of which achieve their optimal implementations based on Quip#. However, CALDERA, despite achieving the highest accuracy, incurs significant latency during inference due to its selection of a larger rank (256-rank in int4). Furthermore, low-rank methods generally underperform compared to rotation-based approaches such as Quip#; nevertheless, with the incorporation of fine-tuning, they can achieve comparable accuracy, demonstrating the robustness of the FLRQ algorithm.

## Downstream task accuracy

We reused the quantization configuration in language generation and performed a zero-shot evaluation on six downstream tasks, including ARC (easy), ARC (challenge), PIQA, OpenBookQA, BOOLQ, and Winogrande, and the results are presented in Table 6. FLRQ’s average accuracy across the

Method	avg. rank	extra. bit	GEN Tasks $\downarrow$		low-rank latency $\downarrow$
			Wiki2	C4	
Quip#	-	-	12.74	16.84	-
FLRQ	40	0.24	14.12	17.81	4.8%
Quip&CALD	256	0.4	8.87	12.02	26.7%
Quip&RILQ	64	0.4	9.64	12.96	7.1%
FLRQ&RILQ	56	0.36	9.78	13.03	6.5%

Table 5: 2-bit PPL and inference latency on LLaMa3-8B, where CALD is short of CALDERA. QUIP# and FLRQ are PTQ quantization methods, while RILQ and CALDERA are low-rank fine-tuning methods.

Method	OPT			Llama2	
	1.3b	6.7b	13b	7b	13b
FP16	48.8%	55.2%	55.6%	62.7%	63.4%
AWQ(4)	47.4%	54.7%	55.7%	62.2%	64.1%
Omni(4)	47.8%	54.9%	55.6%	62.5%	65.0%
FLRQ(4)	<b>48.4%<math>\uparrow</math></b>	<b>55.0%<math>\uparrow</math></b>	<b>55.1%<math>\uparrow</math></b>	<b>62.7%<math>\uparrow</math></b>	<b>65.4%<math>\uparrow</math></b>
AWQ(3)	46.6%	53.2%	53.5%	60.9%	62.7%
Omni(3)	47.4%	53.7%	54.8%	61.1%	63.4%
FLRQ(3)	<b>47.6%<math>\uparrow</math></b>	<b>54.4%<math>\uparrow</math></b>	<b>55.3%<math>\uparrow</math></b>	<b>61.4%<math>\uparrow</math></b>	<b>64.2%<math>\uparrow</math></b>
Omni(2)	41.9%	46.9%	47.3%	50.1%	53.9%
FLRQ(2)	<b>45.5%<math>\uparrow</math></b>	<b>51.5%<math>\uparrow</math></b>	<b>52.3%<math>\uparrow</math></b>	<b>56.4%<math>\uparrow</math></b>	<b>60.4%<math>\uparrow</math></b>

Table 6: Zero-Shot results ( $\uparrow$ ) in an average across six zero-shot tasks. Omni is in short of OmniQuant and the quantization bit is given in parentheses.

six downstream tasks is consistent with the FP16 baseline, showing near-lossless accuracy in 4bit and 3bit quantization, and maintains considerable accuracy at 2 bits.

## The hyperparameters in FLRQ

**The choice of iterations  $it$ :** The accuracy of r1-sketch is determined by the number of iterations  $it$ . We evaluated the convergence and execution efficiency under varying values of  $it$  and the effectiveness of parameter selection  $it$  in the FLRQ method. The evaluation concludes with PPL and execution time in Table 7. The findings indicate that while a higher  $it$  improves the accuracy of R1-Sketch, setting  $it = 2$  in FLRQ is enough. In this case, R1-Sketch only takes **6 GEMV** of  $O(N^2)$  and some  $O(N)$  routines, providing a balance between accuracy and computational efficiency.

## Time efficiency

We evaluated the efficiency of FLRQ from two perspectives: **Quantization Efficiency:** We tested the quantization speed of FLRQ against other PTQ methods, with the results presented in Table 8. In the 4-bit and 3-bit quantization, where accuracy drop is less, we selected GPTQ and LQER algorithms for comparison due to faster quantization speed. However, in the 2-bit scenario, AWQ and LQER cannot maintain accuracy; therefore, we chose the higher-precision PTQ methods OmniQuant and AffineQuant for evaluation. The result

it	OPT-1.3B		OPT-6.7B	
	PPL	Time	PPL	Time
0	16.84	6.1m/1.2s	11.65	26.5m/3.1s
1	15.56	6.1m/1.8s	11.42	26.5m/5.2s
<b>2</b>	<b>15.53</b>	<b>6.1m/2.1s</b>	<b>11.18</b>	<b>26.6m/9.3s</b>
4	15.53	6.1m/3.5s	11.18	26.7m/16.9s
8	15.53	6.2m/6.8s	11.18	27.0m/29.5s
SVD	15.53	8.7m/2.6m	11.18	56.4m/20.3m

Table 7: The PPL and time costs (**FLRQ** total time)/(R1-FLR partial time) of FLRQ with different *it* parameters on 3-bit quantized OPT models under wikitext2 dataset.

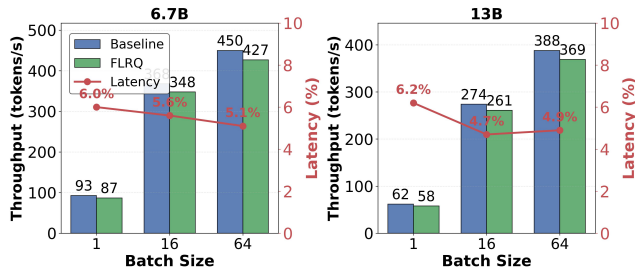


Figure 3: Comparison of Throughput and Latency between Baseline (W4A16) and FLRQ (W4A16+Lora).

shows that, in 3 and 4-bit, FLRQ demonstrated comparable quantization times to methods like AWQ, while being over **30%** faster than LQER, which employs a SVD. Particularly noteworthy is the performance of FLRQ in the challenging 2-bit quantization scenario, where FLRQ exhibited at least a **30%** faster quantization speed compared to OmniQuant, and more than **5** times faster than AffineQuant.

**Inference Efficiency:** We implemented an efficient fusion kernel for low-rank quantization to the AutoGPTQ quantization framework, with the inference results presented in Figure 3. Due to the adoption of the flexible rank selection strategy, FLRQ introduces only a **4%** to **6%** in inference latency.

### Ablation studies

To validate the effectiveness of each strategy within FLRQ, we conducted ablation studies divided into two parts:

- Ablation on R1-FLR:** To demonstrate the effectiveness of **R1-FLR**, we compared it with fixed-rank methods without applying calibration. As shown in Table 9, FLRQ achieves similar or better PPL to fixed-rank methods, yet with a reduced average bit width, indicating higher compression efficiency. Specifically, in the LLaMA2-13B model, FLRQ achieved the same PPL as a fixed rank of 64 while reducing **40%** extra memory costs.
- Ablation on BLC:** We compare the performance with and without **BLC**. The results are presented in Table 10. And the findings indicate that the use of **BLC** further reduces the residual space in low-rank quantization, thereby enhancing the accuracy of low-rank quantization at every bit level. Specifically, in the 2-bit scenario, the **BLC**

technique notably avoids quantization distortion, demonstrating superior performance.

Bit	Method	OPT		LLaMA2	
		1.3b	6.7b	13b	7b
3.4	AWQ	6.7m	28.3m	52.8m	25.2m
	LQER	8.2m	35.3m	1.1h	45.2m
	<b>FLRQ</b>	6.2m	26.6m	51.3m	23.0m
2	Omni	1.2h	3.9h	6.8h	3.1h
	Affine	3.2h	14.4h	25.3h	12.2h
	<b>FLRQ</b>	33.2m	2.5h	4.9h	2.0h

Table 8: The quantization time costs on a single A100 GPU, where ‘m’ stands for minutes and ‘h’ for hours:

Models	RANK=32		RANK=64		FLRQ (NO BLC)	
	avg. bit	PPL	avg. bit	PPL	avg. rank(bit)	PPL
7B	4.32	5.83	4.52	5.73	36.03(4.31)↓	5.74
13B	4.28	4.99	4.44	4.98	21.9(4.24)↓	4.98

Table 9: 4-bit PPL under fixed rank and FLRQ on Wiki2.

The results indicate that **R1-FLR** is capable of significantly reducing the additional overhead associated with low-rank quantization while maintaining quantization accuracy and **BLC** not only improves accuracy across different bit depths but also significantly solves quantization distortion, especially under more challenging 2-bit conditions.

Bit	BLC	OPT		LLaMA2	
		1.3b	6.7b	13b	7b
4	✗	14.58	10.89	10.11	5.55
	✓	14.55↓	10.84↓	10.13	5.55
3	✗	15.80	11.32	10.54	5.89
	✓	15.53↓	11.18↓	10.52↓	5.88↓
2	✗	29.32	17.23	15.41	2.1e6
	✓	22.99↓	14.05↓	12.60↓	9.14↓

Table 10: PPL(↓) on WikiText-2 dataset. Note that “✗” indicates without employing the iterative strategy from **BLC**. Other settings remain consistent with the main experiments.

## Conclusion

In this work, we propose FLRQ, a low-rank quantization method that employs flexible rank selection based on R1-Sketch and iteratively minimizes quantization errors. Compared to other low-rank PTQ, FLRQ features lower additional memory consumption and faster quantization speeds. Extensive experiments demonstrate that FLRQ achieves better precision than several other PTQ methods in model quantization, particularly excelling in 2-bit quantization. Furthermore, we demonstrate the robustness of the FLRQ algorithm and achieve low inference latency through efficient kernel fusion.

## Acknowledgements

This work is partially supported by the Strategic Priority Research Program of Chinese Academy of Sciences (XDB0500101), and the Basic Research Project of the Institute of Software, Chinese Academy of Sciences (ISCAS-JCMS-202304).

## References

Bisk, Y.; Zellers, R.; Le bras, R.; Gao, J.; and Choi, Y. 2020. PIQA: Reasoning about Physical Commonsense in Natural Language. *Proceedings of the AAAI Conference on Artificial Intelligence*, 7432–7439.

Boratko, M.; Padigela, H.; Mikkilineni, D.; Yuvraj, P.; Das, R.; McCallum, A.; Chang, M.; Fokoue-Nkoutche, A.; Kapanipathi, P.; Mattei, N.; et al. 2018. A systematic classification of knowledge, reasoning, and context within the ARC dataset. *arXiv preprint arXiv:1806.00358*.

Clark, C.; Lee, K.; Chang, M.-W.; Kwiatkowski, T.; Collins, M.; and Toutanova, K. 2019. BoolQ: Exploring the surprising difficulty of natural yes/no questions. *arXiv preprint arXiv:1905.10044*.

Dass, J.; Wu, S.; Shi, H.; Li, C.; Ye, Z.; Wang, Z.; and Lin, Y. 2023. Vitality: Unifying low-rank and sparse approximation for vision transformer acceleration with a linear taylor attention. In *2023 IEEE International Symposium on High-Performance Computer Architecture (HPCA)*, 415–428. IEEE.

Ding, Y.; Qin, H.; Yan, Q.; Chai, Z.; Liu, J.; Wei, X.; and Liu, X. 2022. Towards accurate post-training quantization for vision transformer. In *Proceedings of the 30th ACM international conference on multimedia*, 5380–5388.

Frantar, E.; Ashkboos, S.; Hoefer, T.; and Alistarh, D. 2023. GPTQ: Accurate Post-Training Quantization for Generative Pre-trained Transformers. In *The Eleventh International Conference on Learning Representations*.

Gao, L.; Tow, J.; Abbasi, B.; Biderman, S.; Black, S.; DiPofi, A.; Foster, C.; Golding, L.; Hsu, J.; Le Noac'h, A.; Li, H.; McDonell, K.; Muennighoff, N.; Ociepa, C.; Phang, J.; Reynolds, L.; Schoelkopf, H.; Skowron, A.; Sutawika, L.; Tang, E.; Thite, A.; Wang, B.; Wang, K.; and Zou, A. 2024. A framework for few-shot language model evaluation.

Guan, X.; Li, C.-T.; and Guan, Y. 2017. Matrix factorization with rating completion: An enhanced SVD model for collaborative filtering recommender systems. *IEEE access*, 5: 27668–27678.

Halko, N.; Martinsson, P.-G.; and Tropp, J. A. 2011. Finding structure with randomness: Probabilistic algorithms for constructing approximate matrix decompositions. *SIAM review*, 53(2): 217–288.

Hassibi, B.; Stork, D.; and Wolff, G. 1993. Optimal Brain Surgeon and general network pruning. In *IEEE International Conference on Neural Networks*, 293–299 vol.1.

Hubara, I.; Nahshan, Y.; Hanani, Y.; Banner, R.; and Soudry, D. 2021. Accurate post training quantization with small calibration sets. In *International Conference on Machine Learning*, 4466–4475. PMLR.

Ji, H.; and Li, Y. 2014. GPU accelerated randomized singular value decomposition and its application in image compression. *Proc. of MSVESCC*, 39–45.

Kumar, B. 2016. A novel latent factor model for recommender system. *JISTEM-Journal of Information Systems and Technology Management*, 13(3): 497–514.

Kuzmin, A.; Nagel, M.; Van Baalen, M.; Behboodi, A.; and Blankevoort, T. 2023. Pruning vs quantization: Which is better? *Advances in neural information processing systems*, 36: 62414–62427.

Lee, G.; Lee, J.; Hong, S.; Kim, M.; Ahn, E.; Chang, D.-S.; and Choi, J. 2025. RILQ: Rank-Insensitive LoRA-based Quantization Error Compensation for Boosting 2-bit Large Language Model Accuracy. In *Proceedings of the AAAI Conference on Artificial Intelligence*, volume 39, 18091–18100.

Li, M.; Lin, Y.; Zhang, Z.; Cai, T.; Li, X.; Guo, J.; Xie, E.; Meng, C.; Zhu, J.-Y.; and Han, S. 2024a. Svdqnat: Absorbing outliers by low-rank components for 4-bit diffusion models. *arXiv preprint arXiv:2411.05007*.

Li, Y.; Yu, Y.; Liang, C.; Karampatziakis, N.; He, P.; Chen, W.; and Zhao, T. 2024b. LoftQ: LoRA-Fine-Tuning-aware Quantization for Large Language Models. In *The Twelfth International Conference on Learning Representations*.

Lin, J.; Tang, J.; Tang, H.; Yang, S.; Chen, W.-M.; Wang, W.-C.; Xiao, G.; Dang, X.; Gan, C.; and Han, S. 2024. AWQ: Activation-aware Weight Quantization for On-Device LLM Compression and Acceleration. *Proceedings of Machine Learning and Systems*, 6: 87–100.

Liu, Z.; Oguz, B.; Zhao, C.; Chang, E.; Stock, P.; Mehdad, Y.; Shi, Y.; Krishnamoorthi, R.; and Chandra, V. 2024. LLM-QAT: Data-Free Quantization Aware Training for Large Language Models. In Ku, L.-W.; Martins, A.; and Srikumar, V., eds., *Findings of the Association for Computational Linguistics: ACL 2024*, 467–484. Bangkok, Thailand: Association for Computational Linguistics.

Ma, Y.; Li, H.; Zheng, X.; Ling, F.; Xiao, X.; Wang, R.; Wen, S.; Chao, F.; and Ji, R. 2024. AffineQuant: Affine Transformation Quantization for Large Language Models. In *The Twelfth International Conference on Learning Representations*.

Merity, S.; Xiong, C.; Bradbury, J.; and Socher, R. 2016. Pointer sentinel mixture models. *arXiv preprint arXiv:1609.07843*.

Mihaylov, T.; Clark, P.; Khot, T.; and Sabharwal, A. 2018. Can a Suit of Armor Conduct Electricity? A New Dataset for Open Book Question Answering. In *Proceedings of the 2018 Conference on Empirical Methods in Natural Language Processing*.

Osawa, K.; Sekiya, A.; Naganuma, H.; and Yokota, R. 2017. Accelerating matrix multiplication in deep learning by using low-rank approximation. In *2017 International Conference on High Performance Computing & Simulation (HPCS)*, 186–192. IEEE.

Raffel, C.; Shazeer, N.; Roberts, A.; Lee, K.; Narang, S.; Matena, M.; Zhou, Y.; Li, W.; and Liu, P. J. 2020. Exploring the limits of transfer learning with a unified text-to-text transformer. *Journal of machine learning research*, 21(140): 1–67.

Saha, R.; Sagan, N.; Srivastava, V.; Goldsmith, A.; and Pilanci, M. 2024. Compressing large language models using low rank and low precision decomposition. *Advances in Neural Information Processing Systems*, 37: 88981–89018.

Sakaguchi, K.; Bras, R. L.; Bhagavatula, C.; and Choi, Y. 2021. Winogrande: An adversarial winograd schema challenge at scale. *Communications of the ACM*, 64(9): 99–106.

Shao, W.; Chen, M.; Zhang, Z.; Xu, P.; Zhao, L.; Li, Z.; Zhang, K.; Gao, P.; Qiao, Y.; and Luo, P. 2023. Omnipotent: Omnidirectionally calibrated quantization for large language models. *arXiv preprint arXiv:2308.13137*.

Touvron, H.; Martin, L.; Stone, K.; Albert, P.; Almahairi, A.; Babaei, Y.; Bashlykov, N.; Batra, S.; Bhargava, P.; Bhosale, S.; et al. 2023. Llama 2: Open foundation and fine-tuned chat models. *arXiv preprint arXiv:2307.09288*.

Tseng, A.; Chee, J.; Sun, Q.; Kuleshov, V.; and De Sa, C. 2024. Quip#: Even better llm quantization with hadamard incoherence and lattice codebooks. *arXiv preprint arXiv:2402.04396*.

Yao, Z.; Wu, X.; Li, C.; Youn, S.; and He, Y. 2024. Exploring post-training quantization in llms from comprehensive study to low rank compensation. In *Proceedings of the AAAI Conference on Artificial Intelligence*, volume 38, 19377–19385.

Zhang, C.; Cheng, J.; Constantinides, G. A.; and Zhao, Y. 2024. LQER: Low-Rank Quantization Error Reconstruction for LLMs. *arXiv preprint arXiv:2402.02446*.

Zhang, S.; Roller, S.; Goyal, N.; Artetxe, M.; Chen, M.; Chen, S.; Dewan, C.; Diab, M.; Li, X.; Lin, X. V.; et al. 2022. Opt: Open pre-trained transformer language models. *arXiv preprint arXiv:2205.01068*.

**Overall:** Comparison between Traditional Low-Rank Quantization and FLRQ. Typically, low-rank PTQs directly apply scaling and low-rank approximation by SVD to the weight matrices. In contrast, FLRQ utilizes flexible rank selections, activation-based scaling, and iterative Best Low-rank Approximation under Clipping (BLC) algorithm, leading to higher quantization accuracy. Furthermore, R1-Sketch empowers FLRQ to boost efficiency over traditional SVD methods.

**Organization:** In this appendix, we provide further details as follows:

- See Sec.: Presents the details on
  - Analysis of Time Complexity
  - Necessity of R1-Sketch in FLRQ
  - The choice of optimal rank in R1-FLR
- See Sec.: Presents the detail experiments results of FLRQ on
  - Zero-shot tasks
  - Scaling law
  - Apply R1-Sketch in LQER
- See Sec.: Presents detailed information on
  - Hyperparameters of memory threshold  $x$
  - The number of iterations in R1-Sketch  $it$
  - The epoch of BLC

## Detail of FLRQ

### Analysis of Time Complexity

From RSVD, we have R1-Sketch presented as:

$$\begin{aligned} A_L &= QU\Sigma = \frac{\mathbf{Y}}{\|\mathbf{Y}\|} * \{1\} * \|\mathbf{B}\| = \frac{(\mathbf{A}\mathbf{A}^*)^{it}\mathbf{A}\mathbf{S}}{\|(\mathbf{A}\mathbf{A}^*)^{it}\mathbf{A}\mathbf{S}\|} * \frac{\|\mathbf{S}^*\mathbf{A}^*(\mathbf{A}\mathbf{A}^*)^{it}\mathbf{A}\|}{\|(\mathbf{A}\mathbf{A}^*)^{it}\mathbf{A}\mathbf{S}\|} \\ A_R &= \mathbf{V} = \frac{\mathbf{B}}{\|\mathbf{B}\|} = \frac{\mathbf{S}^*\mathbf{A}^*(\mathbf{A}\mathbf{A}^*)^{it}\mathbf{A}}{\|\mathbf{S}^*\mathbf{A}^*(\mathbf{A}\mathbf{A}^*)^{it}\mathbf{A}\|}. \end{aligned} \quad (13)$$

Take  $\mathbf{P} = (\mathbf{A}\mathbf{A}^*)^{it}\mathbf{A}\mathbf{S}$  and  $\mathbf{K} = \mathbf{A}^*\mathbf{P}$ . Therefore,

$$A_L = \frac{\|\mathbf{K}\|}{\|\mathbf{P}\|} \cdot \frac{\mathbf{P}}{\|\mathbf{P}\|} \in \mathbb{R}^{m \times 1}, \quad A_R = \frac{\mathbf{K}}{\|\mathbf{K}\|} \in \mathbb{R}^{1 \times n}. \quad (14)$$

Then the rank-1 matrix  $\mathbf{A}_1 = \mathbf{A}_L \mathbf{A}_R$  corresponds to the matrix spanned by the singular vector associated with the largest singular value of matrix  $\mathbf{A}$ . The same process can then be applied to the residual part  $\mathbf{A} - \mathbf{A}_1$  to obtain the rank-1 matrix corresponding to the next largest singular value. By iterating this process, we can successively construct a rank-r approximation of  $\mathbf{A}$ .

Now we conclude that a rank-1 sketch approximation (R1-Sketch) and have Algorithm.4. Since R1-Sketch is entirely derived from the RSVD algorithm under the rank-1 condition, it maintains the same accuracy and error bounds as the RSVD algorithm.

While the norms of  $\|\mathbf{K}\|$  and  $\|\mathbf{P}\|$  can be efficiently computed with a time complexity of  $O(n)$ . Consequently, the main computational cost of the algorithm is the calculation of  $\mathbf{P}$  and  $\mathbf{K}$ , which is composed entirely of GEMV (matrix-vector multiplication), and with a time complexity of  $O((2it + 2)n^2)$ . As the parameter  $it$  increases, the algorithm achieves higher accuracy at the cost of greater computational overhead. However, in practical applications,  $it$  does not need to be very large (approximately 2) to achieve good approximation results in the context of l1m quantization. We will provide a further discussion Section .

---

### Algorithm 3: R1-Sketch-based Flexible Low-Rank Selection (**R1-FLR**)

---

**Data:**  $\mathbf{W}$ (weight matrix),  $d$ (bits),  $x$ (maximum model size increase)

**Result:**  $\mathbf{W}_L, \mathbf{W}_R$

```

get shape and maximum rank:  $\{m, n\} \leftarrow \mathbf{W}.shape, R \leftarrow \min(m, n);$ 
get origin maximum absolute value:  $maxAbs_0 \leftarrow max(abs(\mathbf{W}));$ 
for  $i = 1$  to  $R$  do
  Obtain the sketch rank-1 matrix corresponding to the largest singular value:  $\{U_1, V_1\} \leftarrow calR1matrix(\mathbf{W});$ 
   $\mathbf{W} \leftarrow \mathbf{W} - \mathbf{U}_1 \cdot \mathbf{V}_1;$ 
  get maximum absolute value now:  $maxAbs \leftarrow max(abs(\mathbf{W}));$ 
  Calculate P, Q, K:  $P \leftarrow maxAbs_0 \leftarrow maxAbs;$ 
   $Q \leftarrow (d + log_2(P))/d;$ 
   $K \leftarrow 1 + (d * r * (m + n))/(m * n));$ 
  Calculate the slope of maxAbs:  $sNow \leftarrow getSlope(maxAbs);$ 
  if  $K > Q$  or  $K > 1 + x$  or  $sNow < t$  then
    | Endloop;
  end
   $\mathbf{W}_L \leftarrow \mathbf{W}_L.append(U_1);$ 
   $\mathbf{W}_R \leftarrow \mathbf{W}_R.append(V_1);$ 
end
return  $\mathbf{W}_L, \mathbf{W}_R$ 

```

---

### Algorithm 4: R1-Sketch-based Flexible Low-Rank Selection (**R1-FLR**)

---

**Data:**  $\mathbf{W}$ (weight matrix),  $d$ (bits),  $x$ (maximum model size increase)

**Result:**  $\mathbf{W}_L, \mathbf{W}_R$

```

for  $i = 1$  to  $R$  do
   $\{U_1, V_1\} \leftarrow calR1matrix(\mathbf{W});$ 
   $\mathbf{W} \leftarrow \mathbf{W} - \mathbf{U}_1 \cdot \mathbf{V}_1;$ 
end
return  $\mathbf{W}_L, \mathbf{W}_R$ 

```

---

### Discussion on the necessity of R1-Sketch

Why is R1-Sketch necessary? Given that the algorithm is derived from RSVD, and its computational accuracy is the same as that of the RSVD algorithm, the necessity of R1-Sketch mainly lies in considerations of computational efficiency. The sole difference

between R1-Sketch and RSVD or truncated SVD is that the construction of the sketch matrix in R1-Sketch is discrete; that is, for each rank, the determination of  $absmax$  or error  $\mathbb{E}$  can be achieved through a single rank-1 approximation. If the condition for optimal rank is met, the computation stops immediately without any redundant calculations.

However, if the SVD algorithm is applied, it requires decomposing the entire matrix. Similarly, using RSVD or truncated SVD requires to specify the rank  $r$  of the approximate matrix beforehand. But before calculating the error or  $absmax$  value, the optimal rank value cannot be known, making it necessary to approximate with a relatively large rank across all layers and then traverse every sub-matrix of this rank- $r$  matrix to determine the best rank. Sub-matrices beyond the best rank are essentially unused, representing redundant computations. In the case of the LLaMA2-7b model, the optimal rank sizes for different layers are shown in Table 11, varying from 0 to 128. Using RSVD would require approximating with a larger rank value (above 128) followed by the application of FLR techniques. Due to BLC technology, FLRQ under low-bit conditions requires more iterations to reduce the residual space, necessitating multiple low-rank approximation functions. Decomposing with a large rank consumes considerable computing resources unnecessarily.

Table 11: In the LLaMA2-7b model, the statistical results of the best rank across different layers.

Rank	0~8	8~16	16~32	32~48	48~64	64~128	avg.rank
Layer-Nums	7	19	44	61	37	5	35.29

For truncated SVD, we set the truncation rank to 128 for models up to 7 billion parameters, and to 256 for the 13 billion parameter model (this setting is due to the best rank for certain layers in the 13 billion model reaching 237). We measured the quantization time, and the results are reported in Table 12. The results show that the computation time using truncated SVD is significantly high, whereas R1-Sketch effectively reduces the computational load, greatly enhancing computational efficiency. This also demonstrates the effectiveness and necessity of R1-Sketch within the FLRQ algorithm.

Table 12: The runtime for model quantization when using Truncated SVD (T-SVD) and R1-Sketch in the FLRQ on different models.

Precision	Method	OPT			LLaMA2		
		1.3b	2.7b	6.7b	13b	7b	13b
3bit,4bit	FLRQ(T-SVD)	16.0m	39.5m	1.4h	3.3h	1.1h	3.1h
	FLRQ(R1-Sketch)	6.2m	12.3m	26.6m	51.3m	23.0m	40.3m
2bit	FLRQ(T-SVD)	1.3h	2.1h	5.9h	12.8h	5.2h	11.3h
	FLRQ(R1-Sketch)	33.2m	1.1h	2.5h	4.9h	2.0h	3.8h

## The choice of optimal rank in R1-FLR

We present the variation curves of low-rank quantization error and  $absmax$  with increasing rank in the LLaMA2-7b model in Figure 4. Across different layers, the error curves are generally smooth but exhibit varying rates of decrease. The  $absmax$  variation curves closely resemble those of the error  $E$ . In most cases, R1-FLR using  $absmax$  can effectively determine an optimal rank. For instance, in *Layer32-down*, using a rank of just 15 achieves nearly a 50% reduction in error, while in *Layer1-k*, a rank of 44 results in an 85% reduction in error.

However, due to the quantization strategy involving repeated iterations and subsequent computations, the  $absmax$  curve does not always perfectly align with the final error curve. For example, in *Layer1-down*, the error is nearly zero at a rank of around 2, with minimal changes thereafter, whereas the  $absmax$  curve continues to show significant decreases around this rank, leading to an estimated optimal rank that is disproportionately high, around 30. Although there are instances where the error curve and  $absmax$  curve do not fit well, the flexible rank selection approach still better accommodates the characteristics of different layers compared to using a fixed rank.

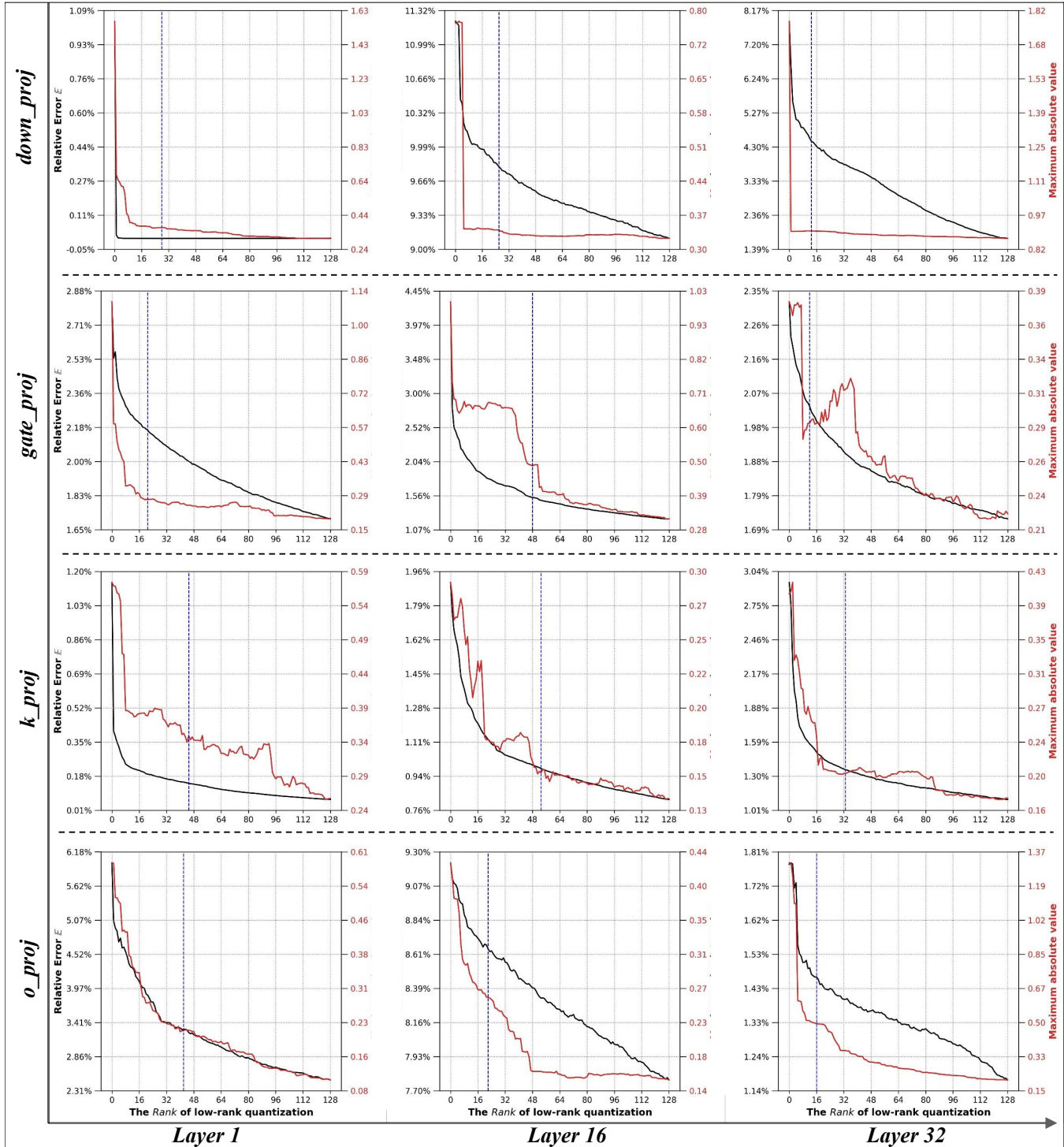


Figure 4: More visualization in LLaMA2-7b on the relationship between rank selection and the error  $\mathbb{E}/\text{absmax}$ , where the blue lines (---) stand for the optimal rank from R1-FLR. Results demonstrate how varying the rank affects the quantization error, providing insights into the trade-offs between different rank choices and their corresponding impact on quantization accuracy.

## Supplementary EXPERIMENT DETAILS

### ZERO-SHOT TASKS

This section contains additional results for zero-shot tasks. Here **OpenbookQA** is in short of **OB-QA**, and **ARC-C**, **ARC-E** stands for **ARC-challenge** and **ARC-easy**. The introduction of the datasets are as follows:

- ARC-Challenge: This dataset contains science exam questions (typically multiple-choice) specifically curated to be difficult for retrieval-based and word co-occurrence methods.
- ARC-Easy: This counterpart contains science questions from the same source (elementary and middle school level) that are more readily answerable by simple information retrieval or shallow methods.
- BoolQ (Boolean Questions): This dataset consists of yes/no questions based on short passages of text. The task requires a model to read a passage and a related question, then determine the correct boolean answer (True/False or Yes/No).
- OpenBookQA: This dataset is built around a "book" of elementary-level science facts. Each question requires the model to use one or more of these core facts in conjunction with common knowledge to perform multi-step reasoning and answer the question correctly.
- PIQA: This dataset focuses on commonsense physical reasoning. It presents questions about the physical world (e.g., "How would one go about hanging a picture?") with two possible answer choices. The goal is to select the more physically plausible or sensible solution.
- Winogrande: This dataset is designed to evaluate commonsense reasoning, specifically coreference resolution, using a Winograd Schema format. It presents sentences with ambiguous pronouns, where resolving the correct referent requires understanding the context and applying real-world knowledge.

Table 13: OPT-1.3b

	OPT-1.3b	ARC-C	ARC-E	BOOLQ	OB-QA	PIQA	Wino	Avg. Acc
4bit	FP16	23.29%	57.03%	57.83%	23.40%	71.60%	59.51%	48.78%
	Omniquant	23.41%	55.33%	56.21%	22.22%	71.13%	58.46%	47.79%
	AWQ	23.31%	53.34%	55.15%	22.40%	71.81%	58.10%	47.35%
	FLRQ	23.81%	57.28%	57.68%	22.00%	71.06%	58.64%	48.41%
3bit	Omniquant	23.13%	54.97%	56.76%	21.32%	70.51%	57.51%	47.37%
	AWQ	21.01%	54.63%	54.16%	22.00%	70.78%	56.88%	46.58%
	FLRQ	22.35%	55.05%	59.82%	20.60%	70.08%	57.77%	47.61%
2bit	Omniquant	19.98%	45.15%	57.76%	16.62%	60.79%	51.33%	41.94%
	FLRQ	22.53%	48.86%	61.28%	17.60%	66.49%	56.51%	45.55%

Table 14: OPT-6.7B

	OPT-6.7b	ARC-C	ARC-E	BOOLQ	OB-QA	PIQA	Wino	Avg. Acc
4bit	FP16	30.46%	65.61%	66.09%	27.60%	76.28%	65.19%	55.21%
	Omniquant	30.62%	65.61%	66.21%	26.77%	75.98%	64.32%	54.92%
	AWQ	30.50%	65.30%	65.20%	26.60%	76.60%	64.20%	54.73%
	FLRQ	29.78%	65.78%	66.64%	27.20%	75.95%	64.88%	55.04%
3bit	Omniquant	29.33%	64.13%	65.12%	24.98%	74.56%	64.04%	53.69%
	AWQ	28.98%	63.76%	64.77%	24.20%	74.24%	63.35%	53.22%
	FLRQ	29.86%	64.27%	65.60%	25.80%	75.73%	64.96%	54.37%
2bit	Omniquant	22.44%	56.76%	56.42%	21.53%	66.77%	57.56%	46.91%
	FLRQ	26.54%	60.35%	63.33%	24.80%	72.69%	61.01%	51.45%

Table 15: OPT-13B

	OPT-13b	ARC-C	ARC-E	BOOLQ	OB-QA	PIQA	Wino	Avg. Acc
4bit	FP16	32.85%	67.09%	65.87%	27.00%	75.84%	65.19%	55.64%
	Omniquant	33.51%	66.78%	66.02%	26.77%	75.47%	65.25%	55.63%
	AWQ	33.20%	66.80%	66.50%	28.00%	75.60%	64.30%	55.73%
	FLRQ	34.04%	66.92%	68.65%	26.80%	75.52%	65.59%	56.25%
3bit	Omniquant	30.87%	65.66%	68.42%	26.13%	75.83%	61.82%	54.79%
	AWQ	30.12%	63.24%	68.12%	24.14%	73.24%	61.88%	53.46%
	FLRQ	30.89%	65.36%	69.57%	26.20%	76.06%	63.77%	55.31%
2bit	Omniquant	20.44%	54.21%	58.32%	22.13%	69.95%	58.89%	47.32%
	FLRQ	27.73%	61.24%	64.53%	24.20%	72.80%	63.30%	52.30%

Table 16: LLaMA2-7B

	LLaMA-2-7b	ARC-C	ARC-E	BOOLQ	OB-QA	PIQA	Wino	Avg. Acc
4bit	FP16	43.43%	76.35%	77.71%	31.40%	78.07%	69.22%	62.70%
	Omniquant	43.32%	76.01%	77.75%	31.50%	77.67%	68.89%	62.52%
	AWQ	43.30%	75.20%	77.30%	31.40%	77.60%	68.20%	62.17%
	FLRQ	43.77%	76.39%	77.61%	31.60%	77.58%	69.14%	62.68%
3bit	Omniquant	40.78%	74.49%	74.28%	31.88%	77.75%	67.64%	61.14%
	AWQ	39.22%	73.88%	74.87%	31.35%	77.24%	68.98%	60.92%
	FLRQ	40.36%	73.95%	75.08%	32.00%	77.53%	69.30%	61.37%
2bit	Omniquant	28.84%	58.12%	60.33%	24.14%	70.17%	59.12%	50.12%
	FLRQ	35.49%	67.72%	70.09%	26.20%	74.48%	64.64%	56.44%

Table 17: LLaMA2-13B

	LLaMA-2-13b	ARC-C	ARC-E	BOOLQ	OB-QA	PIQA	Wino	Avg. Acc
4bit	FP16	49.10%	77.44%	80.71%	35.90%	81.35%	73.89%	66.40%
	Omniquant	47.63%	78.82%	79.13%	33.35%	79.01%	71.89%	64.97%
	AWQ	46.90%	78.90%	77.30%	31.40%	77.60%	72.40%	64.08%
	FLRQ	48.21%	79.97%	79.45%	34.40%	78.56%	71.82%	65.40%
3bit	Omniquant	42.00%	77.94%	79.03%	32.25%	77.98%	71.32%	63.42%
	AWQ	42.04%	77.33%	78.22%	31.85%	76.14%	70.53%	62.69%
	FLRQ	45.22%	78.37%	79.08%	32.80%	78.40%	71.27%	64.19%
2bit	Omniquant	31.33%	62.31%	64.09%	27.52%	72.33%	65.65%	53.87%
	FLRQ	39.16%	72.05%	76.45%	30.20%	76.12%	68.35%	60.39%

## Scaling laws

Quantization is an effective strategy to reduce the total model size, thereby facilitating the deployment of large language models (LLMs) on memory-constrained edge or consumer devices. An excellent quantization algorithm should maintain effective accuracy across a range of models from small to large, meaning that the quantization effectiveness should improve in terms of accuracy as the model size increases across different bit widths. We present the perplexity (PPL) results of Fixed Low-Rank Quantization (FLRQ) across various datasets in Figure 5. The results demonstrate that FLRQ maintains sufficiently impressive scaling effects, particularly achieving comparable performance to 4-bit quantization in terms of the trade-off between model size and PPL with its 3-bit quantization.

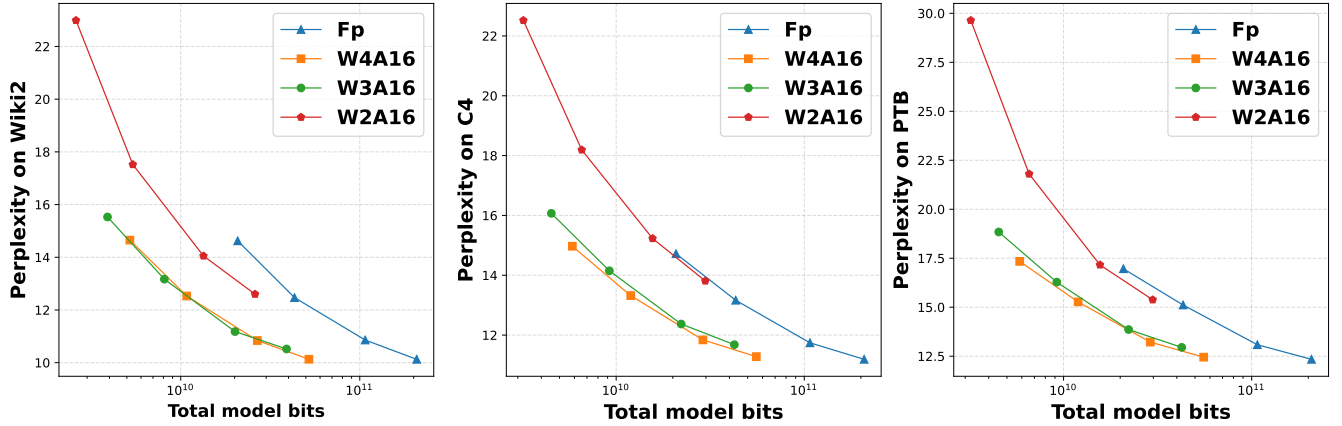


Figure 5: The scaling laws of perplexity under bit-level.

### Apply R1-Sketch in LQER

In this section, we present experiments comparing the original low-rank approximation implementation (`torch.linear.svd`) in the LQER algorithm with its replacement by **R1-Sketch**, evaluating both PPL and execution time in low-rank approximation. The results demonstrate that R1-Sketch significantly improves algorithm execution speed while maintaining lossless performance in terms of PPL.

Table 18: The WikiText2 PPL performance of L<sup>2</sup>QER on different models, with quantization parameters set to W4A16, rank  $r = 32$ , and group size is 128.

Method	OPT		LLaMA-2	
	6.7B	13B	7B	13B
FP16	10.86	10.13	5.48	4.88
L <sup>2</sup> QER-svd	10.99	10.24	5.58	4.96
L <sup>2</sup> QER-sketch	10.99	10.23	5.58	4.96

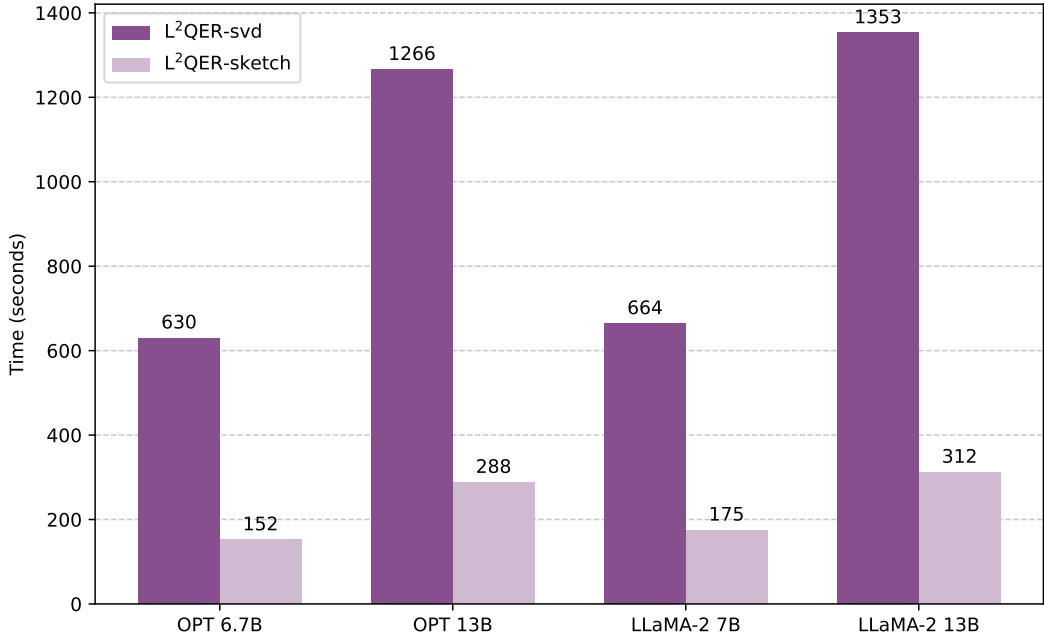


Figure 6: R1-Sketch is an accuracy-preserving low-rank approximation method designed for large-scale model quantization scenarios. Compared to the built-in SVD function in PyTorch, the rank-32 low-rank approximation in L<sup>2</sup>QER achieves a maximum of 4.4× speedup during the approximation stage.

## Detailed experiments on hyperparameter selection

### The setting of memory limit $x$

In FLRQ, we introduced a hyperparameter  $x$  to represent our desired maximum increase in the size of the model. In this context, if the memory usage of the low-rank component larger than  $x$ , it indicates that the additional memory overhead introduced by low-rank components has approached the acceptable maximum size (i.e., the model cannot grow further!). At this point, the iteration process will terminate immediately.

The optimal rank selection strategy in **R1-FLR** is not directly related to  $x$ ; the threshold  $x$  only determines the maximum value for rank selection. We show the rank / extra average bit width of FLRQ at different  $x$  values in Table 19 and actual memory consumption in Table 20 together with Wikitext2-PPL in Table 21.

From the experimental results, it shows that for smaller models (OPT-125M), since the effective rank of the matrix in the quantization scenario is close to the overall size of the matrix, a larger threshold (e.g., 0.4) can lead to higher quantization accuracy but also significantly increases the average number of quantized bits. However, for larger models (OPT-2.7B and more), where the matrix dimensions far exceed the rank of low-rank components extracted by **R1-FLR**, the performance of FLRQ is similar across different thresholds.

From another perspective, as the model size increases, the average number of bits extracted by FLRQ gradually decreases. In the 2-bit, 3-bit, and 4-bit quantization scenarios for the 13B model, the low-rank components only occupy around 0.2 bits. For example, under W4A16G128-OPT13B, the total average number of bits for FLRQ is 4(4bit quantization) + 0.12(low-rank component of FLRQ) + 0.16 (for storing scale and zero with a group size of 128)-*i* **total = 4.28 bits**. Therefore, FLRQ also exhibits excellent scalability from a memory perspective on larger models.

In terms of actual memory consumption, since the quantization does not quantize every weight matrix, FLRQ’s actual memory footprint is less than the average extra bits usage! In the LLaMA2-13B model, at a  $x = 0.2$ , the additional memory usage of FLRQ is only approximately 4% of that in 3-bit quantization and about 6% of that in 2-bit quantization.

For the reasons mentioned above, we uniformly set the threshold  $x = 0.2$  in other experiments. This setting ensures model accuracy across various scales while preventing excessive additional memory consumption.

Table 19: The extracted rank and extra average bit width of FLRQ at different  $x$  values, represented as (rank/extra-avg.bit). The corresponding PPL results can be found in Table 21. In other experiments, the  $x$  value is set to 0.2, with these results highlighted in a darker color.

Bit	x	OPT				LLaMA2		
		125M	1.3B	2.7B	6.7B	13B	7B	13B
4	0.1	12.3/0.36	27.0/0.31	25.4/0.26	27.0/0.16	26.4/0.12	34.9/0.20	38.2/0.18
	0.2	19.9/0.64	30.5/0.34	29.6/0.27	27.1/0.16	27.0/0.12	36.1/0.21	38.6/0.18
	0.4	27.7/0.77	31.32/0.35	32.3/0.28	27.8/0.16	27.2/0.12	36.4/0.21	38.7/0.18
3	0.1	8.3/0.28	21.0/0.26	24.4/0.23	26.6/0.15	26.5/0.12	35.1/0.20	38.0/0.18
	0.2	16.1/0.54	28.8/0.33	28.9/0.26	27.7/0.16	26.4/0.12	35.8/0.21	38.4/0.18
	0.4	25.1/0.75	29.6/0.34	30.2/0.27	27.8/0.16	26.4/0.12	36.0/0.21	38.5/0.18
2	0.1	5.6/0.19	18.0/0.19	18.4/0.18	27.0/0.16	27.3/0.12	36.3/0.22	40.3/0.19
	0.2	10.4/0.38	27.6/0.33	30.9/0.29	32.7/0.19	33.6/0.15	39.2/0.24	41.9/0.20
	0.4	21.2/0.70	28.7/0.34	32.1/0.30	34.1/0.20	33.9/0.15	40.1/0.25	42.1/0.20

Table 20: The memory costs of FLRQ under different values of  $x$ , where  $x = 0$  corresponds to no additional low-rank matrices being used, i.e., the original W(2,3,4)G128 quantization.

Bit	x	OPT				LLaMA2		
		125M	1.3B	2.7B	6.7B	13B	7B	13B
fp16		313MB	2.52GB	5.21GB	12.6GB	25.71GB	13.48GB	26.03
4	0	125MB	1050MB	1.84GB	4.22GB	7.63GB	3.89GB	7.25GB
	0.1	128MB	1095MB	1.91GB	4.32GB	7.79GB	4.07GB	7.46GB
	0.2	130MB	1101MB	1.92GB	4.32GB	7.79GB	4.08GB	7.47GB
3	0.4	132MB	1102MB	1.93GB	4.32GB	7.79GB	4.08GB	7.47GB
	0	114MB	859MB	1.53GB	3.09GB	5.73GB	3.08GB	5.43GB
	0.1	116MB	894MB	1.60GB	3.20GB	5.92GB	3.22GB	5.57GB
2	0.2	118MB	907MB	1.61GB	3.21GB	5.92GB	3.27GB	5.64GB
	0.4	120MB	908MB	1.62GB	3.21GB	5.92GB	3.27GB	5.64GB
	0	101MB	713MB	1.20GB	2.30GB	4.21GB	2.27GB	3.93GB
2	0.1	102MB	743MB	1.25GB	2.42GB	4.4GB	2.46GB	4.15GB
	0.2	104MB	759MB	1.29GB	2.44GB	4.45GB	2.47GB	4.16GB
	0.4	106MB	761MB	1.29GB	2.45GB	4.45GB	2.48GB	4.16GB

Table 21: The PPL( $\downarrow$ ) of FLRQ on Wikitext2 at different  $x$  values. The corresponding rank/extra-avg.bit results can be found in Table 19. In other experiments, the  $x$  value is set to 0.2, with these results highlighted in a darker color.

Bit	x	OPT				LLaMA2		
		125M	1.3B	2.7B	6.7B	13B	7B	13B
4	0.1	30.31	14.69	12.61	10.84	10.15	5.56	4.94
	0.2	28.65	14.65	12.53	10.84	10.13	5.55	4.94
	0.4	26.98	14.65	12.52	10.84	10.13	5.55	4.94
3	0.1	34.15	15.78	13.29	11.19	10.60	5.89	5.17
	0.2	32.55	15.53	13.17	11.18	10.59	5.88	5.16
	0.4	31.13	15.52	13.12	11.18	10.59	5.87	5.16
2	0.1	121.31	28.84	17.63	14.13	12.71	9.18	6.81
	0.2	79.36	22.99	17.52	14.05	12.60	9.14	6.78
	0.4	54.48	22.96	17.50	14.05	12.60	9.14	6.77

## The choice of iterations $it$

In addition to the PPL in the main experimental section, the effect of the  $it$  parameter can be observed. A critical basis for rank selection in the FLRQ algorithm is the  $absmax$  value of the matrix. To provide a clear visualization of the effects of the **R1-Sketch** algorithm at various iteration parameters, we also show the variation curve of the  $absmax$  extraction effect of the weight matrix in the LLaMA2 and OPT model family with  $it$  parameters. The results are presented from Fig 7 to Fig 12, which can also demonstrate the statement in main experiment,  $it$  can converge completely when it is around 2, and the approximate accuracy is close to the SVD method.

**Visualization of different  $it$  at  $absmax$  in different ranks:**

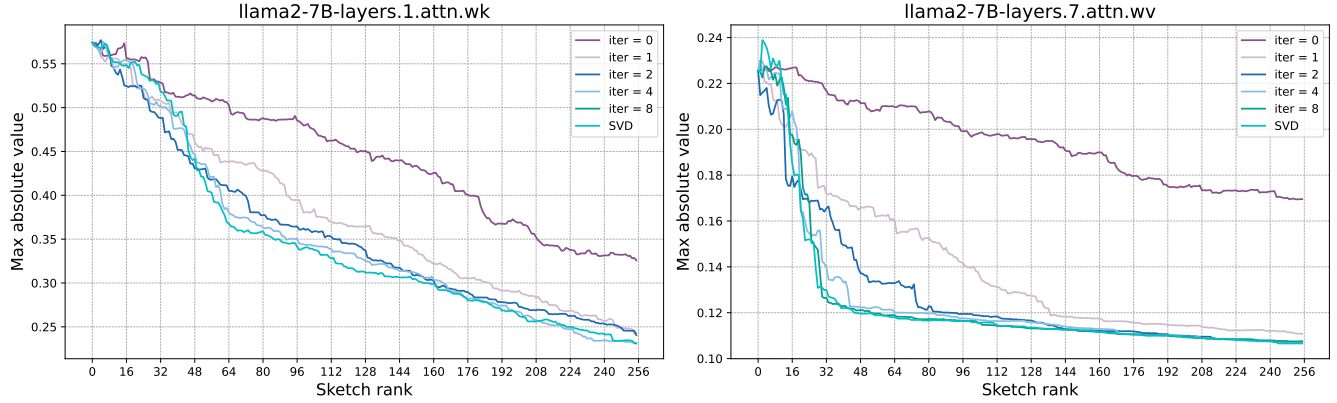


Figure 7: Llama2-7B results

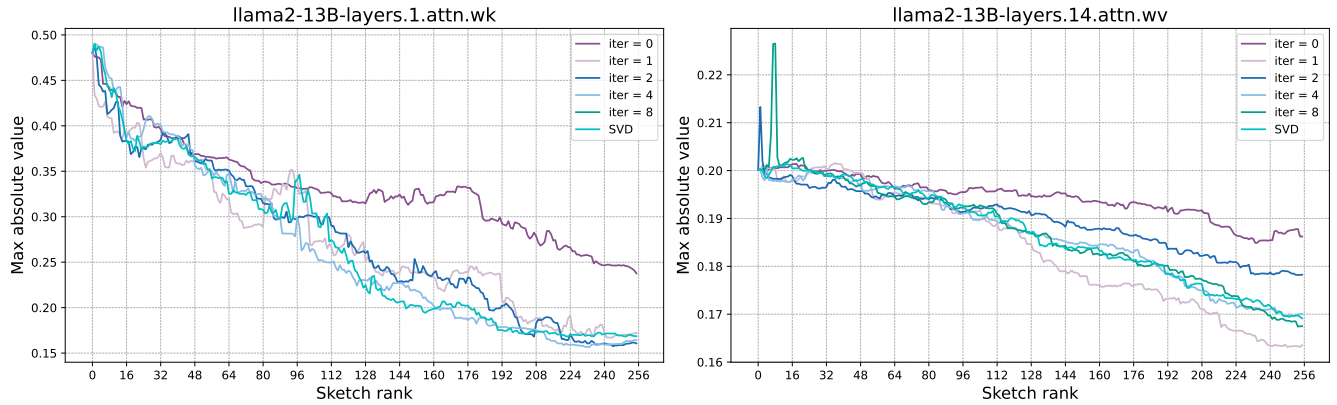


Figure 8: Llama2-13B results

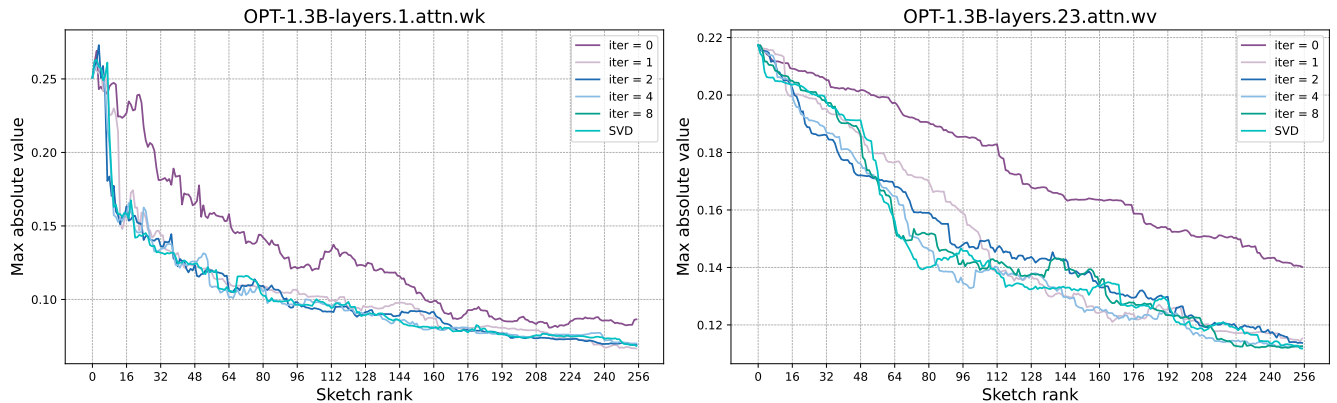


Figure 9: OPT-1.3B results

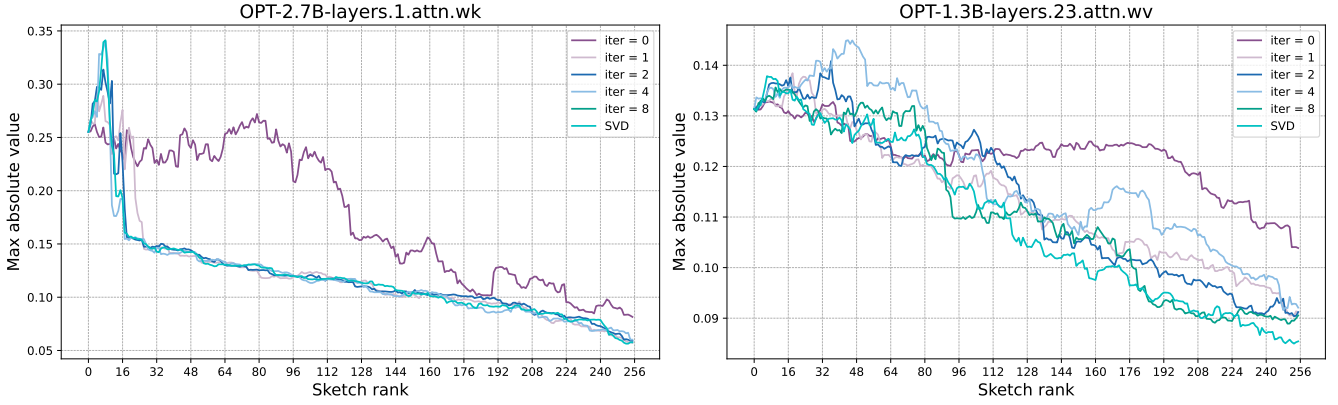


Figure 10: OPT-2.7B results

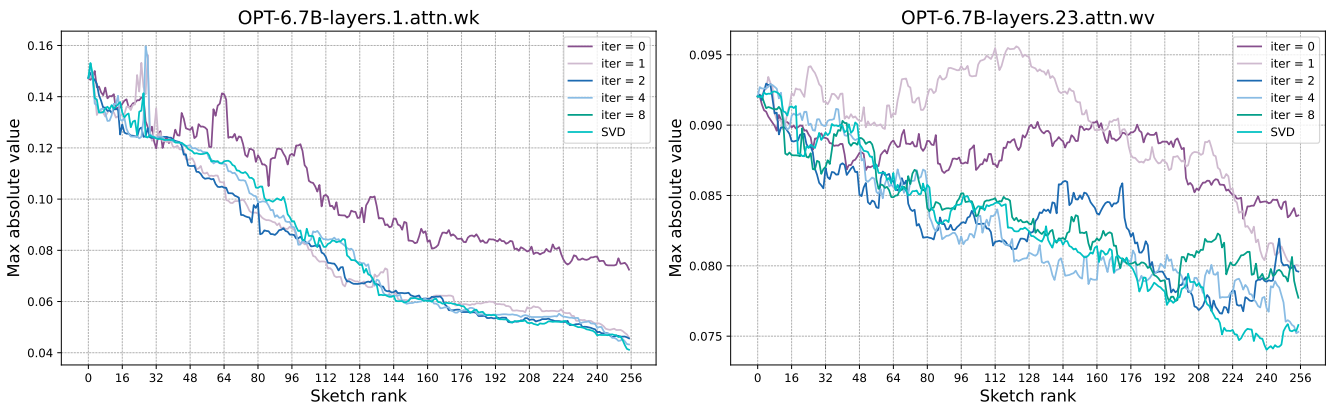


Figure 11: OPT-6.7B results

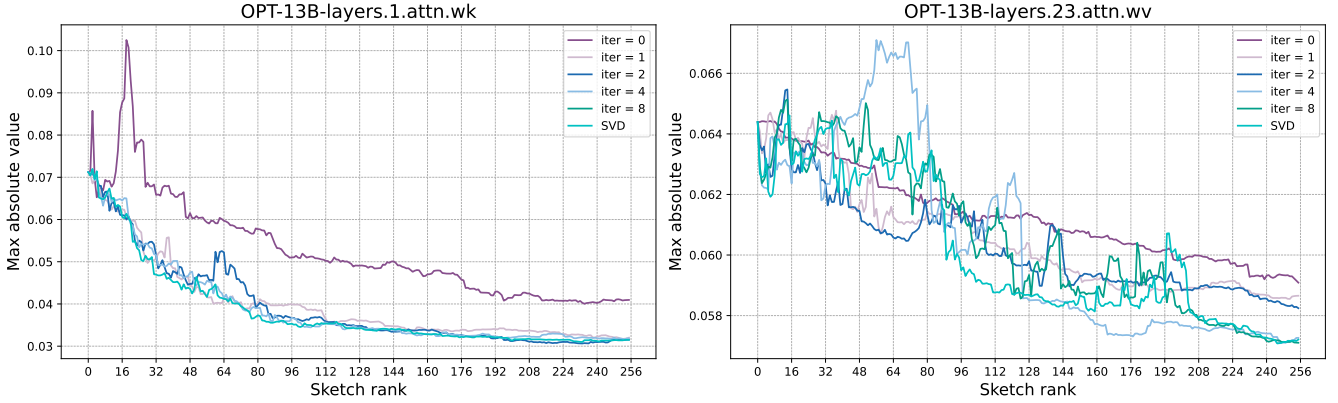


Figure 12: OPT-13B results

### The epoch of BLC

Since BLC reduces quantization error by alternately updating  $W_r$  and  $W_q$  in iterative steps, the final accuracy of the algorithm is related to the number of epochs. A larger number of epochs corresponds to higher accuracy but also increases quantization time. The error reduction curve with respect to iterations is shown in Figure 13, where the error reduction is significantly more pronounced at 2-bit, decreasing by approximately an order of magnitude within 32 epochs, while at 3-bit and 4-bit, the reduction is at most twofold. From the overall model perspective of PPL in Table 22, this corresponds to the BLC algorithm converging within 1 iteration at 3-bit and 4-bit, whereas at 2-bit, approximately 20 iterations are required to achieve optimal accuracy. This also aligns with the results in the quantization time table in the main text, indicating that 2-bit requires more quantization time.

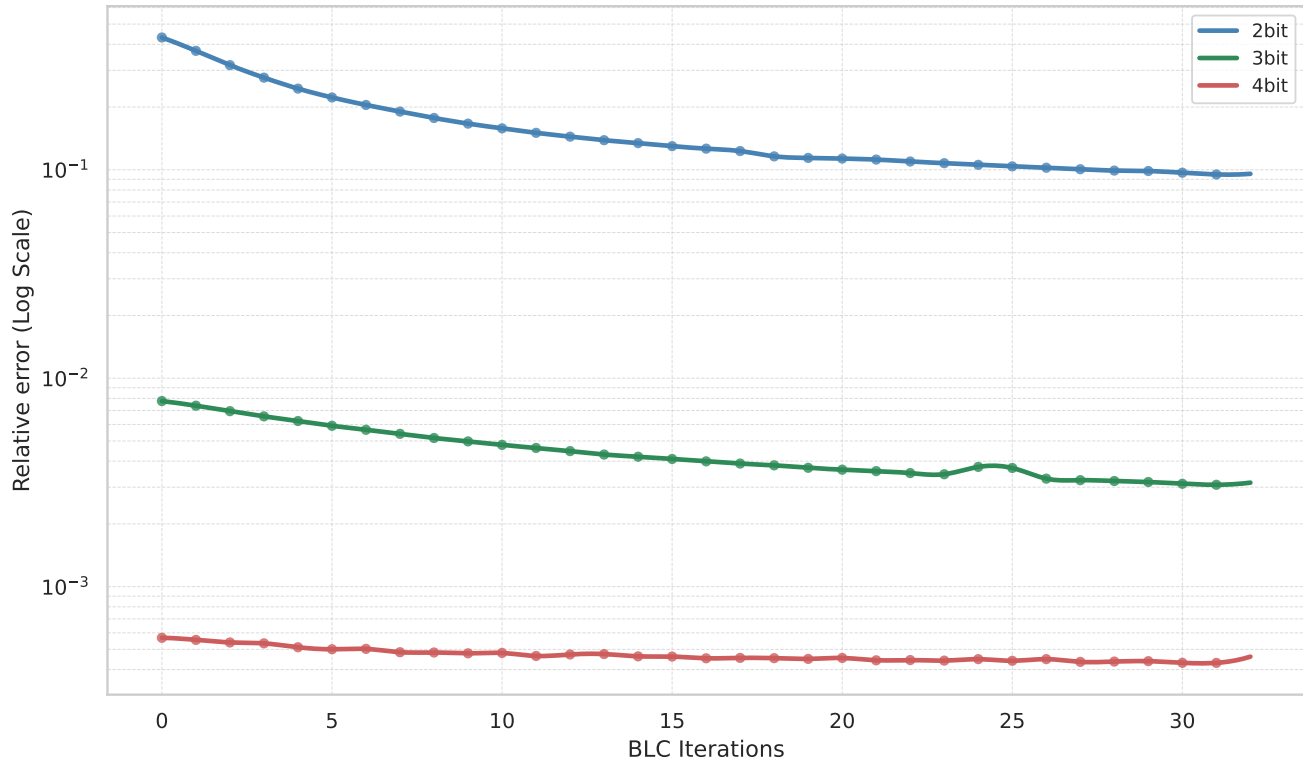


Figure 13: The error curves during BLC iterations at different bit levels.

Table 22: OPT-6.7b Wiki2 PPL at different BLC.

Bit	Epoch				
	1	5	10	20	30
4	<b>10.84</b>	10.84	10.84	10.84	10.84
3	<b>11.18</b>	11.18	11.17	11.17	11.17
2	16.88	15.13	14.09	<b>14.05</b>	14.05